

# The effect of transverse shear on the longitudinal compressive strength of fibre composites

TSU-WEI CHOU

*Mechanical and Aerospace Engineering Department, University of Delaware, Newark, Delaware, USA*

A. KELLY

*Vice-Chancellor's Office, University of Surrey, Guildford, UK*

Experimental work on glass/epoxy composites shows that the compressive strength is sensitive to the method of gripping, that the failure mode in compression varies with fibre volume fraction, and that bending of the specimen may occur as a result of misalignment. Some aspects of these observations are examined. The critical Euler buckling load is significantly reduced if transverse shear occurs. The buckling load depends on specimen dimensions and a good deal of scatter results from this. The predicted compressive strength taking into account the effect of transverse shear and specimen geometry includes the experimental results within a wide scatter band. The present analysis based upon the macro-buckling of the specimen, reproduces some predictions of compressive strength based upon the micro-buckling of fibres.

## 1. Introduction

Extensive work on the compressive strength of composites indicates three major failure modes: fibre buckling, shear failure, and interfacial failure. A review of the state-of-the-art of this subject can be found in [1].

The lack of knowledge of the variation of compressive strength with fibre volume content in a systematic manner, and the sensitivity of measured compressive strength to test fixtures, have together prompted a recent experimental study of these factors. A summary of the experimental work is given in Section 2 and an additional result presented. A theory of the influence of transverse shear on compressive strength is presented in Section 3 and compared with experimental results in Section 4.

## 2. Previous experimental work

Unidirectional glass/epoxy composite specimens were fabricated over a wide range of fibre volume loading [1]. The non-treated E-glass fibre was supplied by Owens-Corning in the form of a

continuous strand. The strand contains 100 filaments with a density of  $2.54 \text{ g cm}^{-3}$ . The PR-288 epoxy film made by 3M Co. was used as the matrix material. It has room temperature tensile strength of 58 MPa and tensile modulus of 3447 MPa. The composite specimens were prepared by first fabricating sheets of pre-pregs using the filament winding technique. The pre-pregs were subsequently laid up by hand to the desired thickness and fibre volume content and cured in an autoclave.

The volume fraction of fibre in the unidirectional laminate was controlled by a combination of the following three methods. The first (the easiest) was to vary the traverse speed of the lathe used for filament winding. The second was to change the number of epoxy sheets used between the pre-pregs; the third was to change the amount of bleeder cloth used in the curing process and therefore the amount of epoxy bled off the curing packet. It is not at all easy to produce specimens of a constant thickness and of varying volume fraction and vice versa.

Composite panels with fibre volume loading ranging from 11% to 58% were made. Compression test specimens were cut from the panels using a diamond blade rotary saw. Scotch-ply fibre glass end-tabs were mounted onto some specimens using the Eccobond 45 epoxy adhesive system of Emerson and Cumings, Inc. Some of the specimens from each panel were instrumented with electrical resistance strain gauges.

Two types of compression test fixtures were used in the experiments. These were the fixtures developed by the IIT Research Institute (IITRI) [2] and the British Royal Aircraft Establishment (RAE) [3]. The IITRI compression test makes use of trapezoidal wedge grips to apply the compressive load and the specimens for this test fixture were mounted with end-tabs. Slippage of the specimens is prevented by bolting across the end-tabs. Lateral alignment of the top and bottom parts of the IITRI fixture is accomplished by the use of parallel roller bushings and corresponding bushing shafts; rollers are used to provide lateral support. The RAE compression fixture uses rectangular test specimens without end-tabs. Each specimen in this case is tightly fitted into the slots of two aluminium blocks with parallel top and bottom surfaces; Eccobond 45 adhesive was used in the slots. The end fittings transfer the applied load to the specimen and prevent the specimen ends from brooming.

The IITRI specimen size is 1.6 to 2.6 mm × 6.4 mm × 127 mm with a gauge length of 12.7 mm. The dimensions of the RAE specimen are 1.3 to 2.1 mm × 19.1 mm × 38.1 mm and also a gauge length of 12.7 mm. The slenderness ratios (see Section 3) of the IITRI specimens, therefore, were between 13.75 and 8.46 and those of the RAE specimens between 33.8 and 20.95. The compression tests were run on an Instron Model TT-D Universal Testing Machine. The cross-head speed of the machine was set at 0.2 mm min<sup>-1</sup>.

A least-square analysis of the data gave the relation between composite axial Young's modulus,  $E_c$ , and fibre volume fraction,  $V_f$ , as:

$$E_c(\text{GPa}) = 2.76 + 79.3 V_f. \quad (1)$$

This result is in reasonable agreement with a "rule of mixtures" based upon the tensile modulus of the fibre and compressive modulus of the matrix:

$$E_c(\text{GPa}) = 3.45 + 68.95 V_f. \quad (2)$$

The variation of compressive strength of the

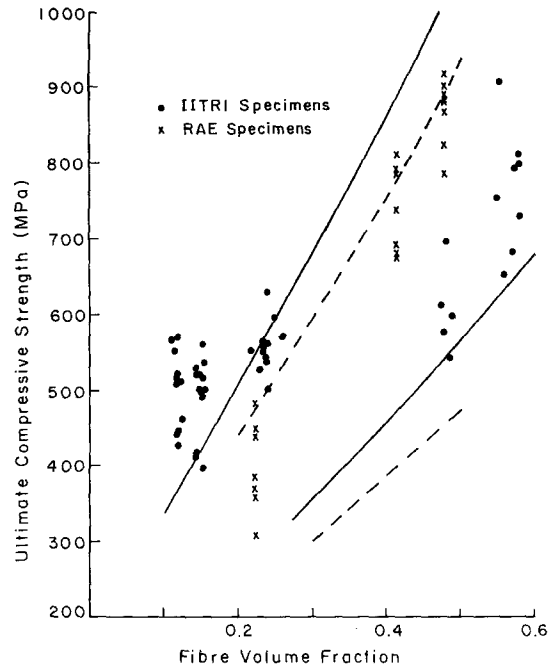


Figure 1 Compressive strength of composites obtained from IITRI test fixture, and RAE test fixture. Solid lines (IITRI) and broken lines (RAE) are the predictions based upon Equation 5 for the upper and lower limits of slenderness ratio.

composites with fibre volume fraction is shown in Fig. 1. The results clearly demonstrate the dependence of composite compressive strength on the method of gripping the specimen although the scatter of results at a given volume fraction is very large. Part of this scatter is due to the fact that it is not easy to make specimens of a given volume fraction and a given thickness. The RAE specimens show higher strength at high volume fraction and lower strength at lower volume fraction than the IITRI specimens. The failure mode of the composites varies with fibre volume content, but a final shear failure is the dominant mode [1].

We believe that the initial failure of the specimens in compression is governed by buckling of the specimens due to their low resistance to transverse shear. The resistance to such buckling is affected by the specimen dimension only through the slenderness ratio ( $l/r$ ) =  $2\sqrt{3}l/t$  ( $l$  = length,  $t$  = thickness) and is independent of specimen width (Section 3). The following experiment was intended to examine the effect of specimen width and, hence of cross-sectional area. Unidirectional E-glass/epoxy composites were fabricated from tape pre-pregs (HY-E 9034C) supplied by Fiberite. Fifteen tapes are used and

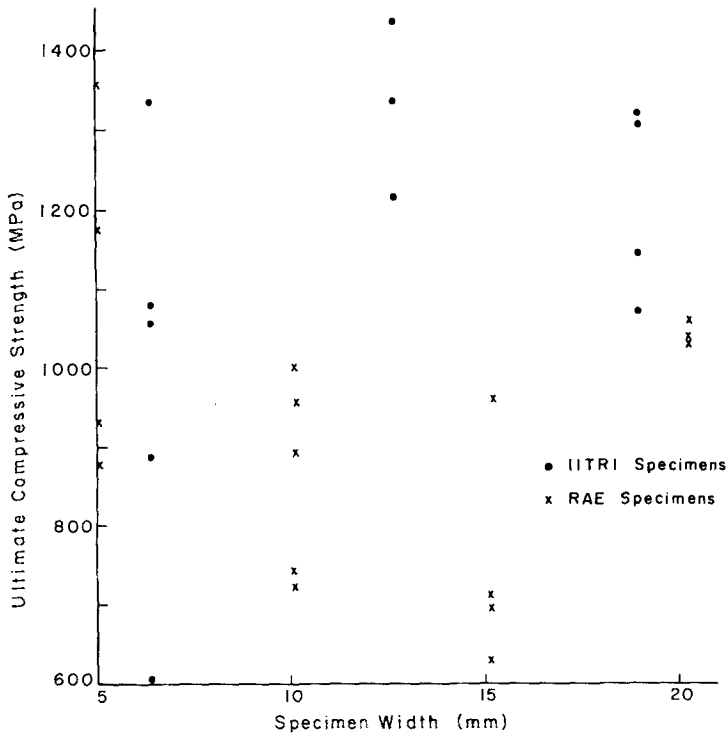


Figure 2 Variation of compressive strength with specimen width.

the procedure of panel fabrication was the same as that described in [1]. A fibre volume fraction of 65% was achieved. The thickness of the specimen so produced varied in the range of 2.0 to 2.3 mm. Also  $l = 7.6$  mm (IITRI) and 12.7 mm (RAE). The variation in slenderness ratio is not large (11.5 to 13.1 for IITRI specimens and 19 to 22 for RAE specimens). Test specimens were cut from the panels at different widths, namely 6.4, 12.7 and 19.1 mm for IITRI specimens and 5.1, 10.2, 15.2 and 20.3 mm for RAE specimens.

The variation of ultimate compressive strength with specimen width is shown in Fig. 2. There is a large scatter of the results. There is no definite indication of a dependence of compressive strength upon specimen width. Equation 5 below indicates a dependence of the buckling stress on  $(l/r)^2$ . The variation of slenderness ratio between specimens can account for a variation of measured initial buckling stress by 34% for a given width. Although this would not account for all of the scatter it does so for a large part of it.

### 3. Theory

The ultimate strength data of [1] show a great deal of scatter. It was also noted that the stress-strain curves of the specimens showed deviation from the initial slope, which is not typical in glass/epoxy composites under tension. This effect is

believed to be caused by the bending of the specimen due to misalignment between the loading axis and the centre line of the specimen. The misalignment can be induced by a number of factors including the poor machining of the specimens, inadequate design of the test fixtures, and defects in the specimens (fibre alignment, local inhomogeneity, etc).

The structural stability of specimens under compressive loading is usually checked by the Euler equation for column buckling. In highly anisotropic materials such as unidirectional fibre composites Euler's prediction, if unmodified, overestimates the compressive strength because the axial Young's modulus of the composites is much greater than the axial shear modulus, by one or two orders of magnitude. The increased deformation due to the deflection due to shear leads to a lower resistance of composites to buckling as has been pointed out by Paton [4]. In view of the fairly uniform distribution of fibres [1] it is reasonable to assume that the specimens possess transverse isotropy with the isotropic planes normal to the loading axis.

The effect of axial or transverse shear on the compressive failure of a composite can be analysed [5] using the following notation:  $P_e$  = Euler critical load,  $P_{cr}$  = critical load under the effect of shearing force,  $n$  = a numerical factor; 1.2 for

rectangular cross-section and 1.11 for circular cross-section,  $t$  = specimen thickness,  $A$  = specimen cross-sectional area,  $l$  = specimen gauge length,  $I$  = second moment of area,  $E_c$  = axial Young's modulus of the unidirectional composite,  $G_c$  = axial shear modulus of the unidirectional composite,  $\sigma_{cr}$  = critical shear stress under the effect of shearing force,  $r = \sqrt{I/A}$ ,  $G_f$  = fibre shear modulus,  $G_m$  = matrix shear modulus,  $V_f$  = fibre volume fraction,  $V_m$  = matrix volume fraction,  $l/r$  = column slenderness ratio =  $2\sqrt{3}(l/t)$ .

The critical load on a composite column, taking into account the deformation due to shear, is given by:

$$P_{cr} = \frac{P_e}{1 + nP_e/AG_c} \quad (3)$$

where

$$P_e = cE_c I/l^2, \quad (4)$$

and  $c$  is a constant determined by the end constraints of the specimen, with the values of 2.47, 9.87 and 20.2, respectively, for the idealized end conditions of clamped-free, hinged-hinged, and clamped-hinged. The Euler critical load is reduced by the factor  $1/(1 + nP_e/AG_c)$ .

The critical compressive stress of the specimen is then:

$$\sigma_{cr} = \frac{cE_c/(l/r)^2}{1 + [cnE_c(l/r)^2G_c]} \quad (5)$$

Equation 5 can be simplified by considering the limiting case where:

$$\frac{cnE_c}{(l/r)^2G_c} \gg 1. \quad (6)$$

This condition is achieved in highly anisotropic composites ( $E_c/G_c \gg 1$ ) and for relatively short specimens ( $l/r$  small, so that tendency to uncorrected Euler buckling is also small). Under the condition of Equation 6,

$$\sigma_{cr} \cong \frac{G_c}{n}. \quad (7)$$

Two expressions of  $G_c$  can be adopted, namely,

$$G_c = \frac{G_m G_f}{V_m G_f + V_f G_m}, \quad (8)$$

based upon a model of fibre and matrix in parallel, and:

$$G_c = G_m \frac{V_m G_m + (1 + V_f)G_f}{(1 + V_f)G_m + V_m G_f} \quad (9)$$

adopted from [6] as a better estimate. By further assuming  $G_f \gg G_m$ ,  $\sigma_{cr}$  can be expressed as

$$\sigma_{cr} = \begin{cases} \frac{G_m}{nV_m} & (10) \\ \frac{G_m}{nV_m} (1 + V_f) & (11) \end{cases}$$

by using Equations 8 and 9 in [7].

Equation 10, apart from the factor  $1/n$ , is the same as Equation 29 of [7], which assumes that the composite fails by the "shear mode" (shearing of the matrix) of microbuckling. Furthermore, Equation 10 is identical to Equation 7 of [8] for  $G_f \gg G_m$  (except for the factor of  $1/n$ ) which was derived by assuming the continuity of shear stress and strain compatibility at the fibre-matrix interface, and by equating the total shear and bending strain energies in the fibre and matrix to the work done by the externally applied forces.

#### 4. Comparison of theory with experiment

The applicability of the above analysis can be compared with the experimental data of [1] obtained using both IITRI and RAE test fixtures. Equation 1 is adopted for the axial Young's modulus of the composite. The following information is relevant:  $G_f = 33$  GPa,  $G_m = 1$  GPa,  $l = 6.35$  mm (IITRI), and 12.7 mm (RAE), and  $G_c$  was calculated from Equation 9.

A feature of the IITRI fixture is the addition of rollers at the mid-point of the gauge length to provide lateral support to the specimen. Consequently, the value of  $l$  used is half of the specimen gauge length.

The parameter  $c$  cannot be determined analytically because of the lack of knowledge of the exact nature of end constraint on the specimens. For this reason it was necessary to determine experimentally the  $c$  values for the IITRI and RAE specimens. Specimens of 2024-T4 aluminium were fabricated with the same dimensions as the IITRI and RAE composite specimens. Aluminium was chosen because its Young's modulus is comparable to that of the composite. The aluminium specimens were then tested in the IITRI and RAE fixtures and the loads at which they buckled were noted. From the knowledge of the buckling loads the constant  $c$  could then be determined using Equation 4. The  $c$  values of 3.34 and 16.14 were obtained for the IITRI and RAE specimens, respectively. By comparing these to the idealized end constraints, it appears that the IITRI specimens lie inbetween the clamped-free and hinged-hinged conditions

whereas the RAE specimens fit inbetween the hinged-hinged and clamped-hinged conditions.

The calculations of the critical buckling stress including transverse shear, Equation 5, are compared with experiment in Fig. 1. Because of the variation in specimen thickness two lines, corresponding to the upper and lower limits of slenderness ratio, are drawn for each type of fixture. The analysis coincides rather better with the experimental findings of the RAE specimens. The prediction of the bounds for the IITRI specimens are less satisfactory at low volume fractions. This is consistent with the observations in [1] since IITRI specimens at low fibre content failed by crushing.

It is probable that the final failure mode derived in [1] is consistent with failure of the specimen starting by macroscopic buckling. If the specimen is compressed parallel to a set of perfectly parallel fibres there are no transverse shear stresses parallel and perpendicular to the fibres. As the specimen buckles these shear forces become larger and therefore it is no surprise that many specimens appear to fail in a shear mode.

The compressive strength of PR-288 epoxy has been measured using RAE specimen design and the average value of three tests is 327 MPa. Equation 5 indicates a variation of buckling stress with volume fraction of fibres, for a given slenderness ratio, through the variation of  $E_c$  and  $G_c$  with fibre content. At low fibre contents the results should extrapolate to the buckling load of the resin alone.

## 5. Conclusions

(1) Any transverse shear deformation is detrimental to the compressive strength of unidirectional fibre composites because of their high anisotropy. The present investigation has demonstrated the importance of the effects of transverse shear on a *macroscopic* scale, an effect emphasized to be of importance by Paton [4] at slenderness ratios the same or slightly larger than those used here. Paton only tested specimens with a single volume fraction of fibres and found that failure was governed by

the (shear corrected) Euler buckling at slenderness ratios greater than about 20. This is consistent with what we have found for RAE specimens over a whole range of volume fractions. By waisting specimens of the RAE type so as to obtain *smaller* slenderness ratios than those used here, Ewins and Ham [9] consistently obtained a failure in compression which is not governed by Euler instability and so represents a property of the material.

(2) The present analysis, based upon the macro-buckling of the specimen, reproduces some compressive strength predictions derived by others based upon micro-buckling of the fibres. The inclusion of the factor  $1/n$  in fact gives results a little better than those of [7] and [8].

## Acknowledgements

We wish to thank J. R. Vinson, W. B. Stewart and J. Richie for helpful discussions and Bill Davis of 3M Co. for supplying the epoxy material.

## References

1. T. W. CHOU, W. B. STEWART and M. G. BADER, 'On the Compressive Strength of Glass-Epoxy Composites' in "New Developments and Applications in Composites", (TMS-AIME, 1979).
2. K.E. HOFER Jr, Technical Report, IIT Research Institute, Chicago, Illinois (1975).
3. P. D. EWINS, TR-71217, Royal Aircraft Establishment (1971).
4. W. PATON, "Effective Structural Use of grp and cfrp" in Composites Standards Testing and Design - Conference Proceedings NPL Conference, April 1974 (IPC Science and Technology Press, Guildford, 1974) p. 36.
5. S. P. TIMOSHENKO and J. M. GERE, "Theory of Elastic Stability (McGraw-Hill, New York, 1961) particularly p. 132 *et seq.*
6. B. W. ROSEN, *Composites* 4 (1973) 16.
7. B. W. ROSEN, in "Fiber Composite Materials" (American Society for Metals, Metals Park, Ohio, 1965) p. 37.
8. S. V. KILKARNI, J. S. RICE and B. W. ROSEN, *Composites* 6 (1975) 217.
9. P. D. EWINS and A. C. HAM, Paper no 74-353, AIAA/ASME 15 Structures Conference, Las Vegas, April (1974).

Received 13 June and accepted 2 July 1979.